PHOTOCATALYTIC DEGRADATION OF ORGANIC POLLUTANTS FROM WATER

Dilip Harijan[1], Priyanka Save[2*], Shashwati Pradhan[3]

[1]Department of Chemistry, Abhinav Degree College,Bhayandar (E)
[2]Department of Chemistry, St.John College of Humanities and Sciences ,Palghar (E)
[3]Department of Chemistry, R.D.National College,Bandra (W)

Keywords

Photocatalysis, Semiconductor, Band gap energy, Solar energy, Visible light absorption, Water splitting, pollutant degradation

Received - *26th June 2025*

Online Published - *27th September 2025*

Abstract

Solar energy harvesting through semiconductor-based photocatalysts has emerged as a promising approach for applications such as solar power generation, water splitting, and the degradation of waterborne pollutants. Photocatalysis operates on the principle of photon-induced excitation of electrons from the valence band (Ev) to the conduction band (Ec) when the incident photon energy (hv) equals or exceeds the band gap energy (Eg) of the material. The generated electron-hole pairs (e^-/h^+) act as strong reducing and oxidizing agents, respectively. While many photocatalysts effectively absorb ultraviolet (UV) light (~390 nm), this only represents a small fraction (~5%) of the solar spectrum. Therefore, significant research is being directed toward extending photocatalytic activity into the visible spectrum (400–750 nm) through strategies such as metal/nonmetal doping, spectral sensitization with dyes or polymers, and the use of narrow-band-gap semiconductors as photosensitizers. However, the efficiency of photocatalysis is often limited by factors such as nanoparticle aggregation and charge carrier recombination. The formation of mesoporous structures and enhanced charge separation/migration have shown promise in overcoming these limitations and improving photocatalytic performance. This work reviews the fundamental mechanisms and current advancements in semiconductor-based photocatalysis aimed at enhancing solar energy utilization.

Introduction

Solar energy is a clean, sustainable, and abundant resource. The earth receives energy of about 3×1024 joules in a year from the sun, which is higher than the global energy consumption. It consists of 5 % UV (300 nm-400 nm), 43 % visible (400 nm-700 nm) and 52% near infrared (700 nm-2500 nm) [1]. Solar energy consists of many particles called photons. The energy of each photon depends on wavelength (λ) and given by, E = hν = hc / λ, where h is Planck's constant (6.626 x10-34Js) and c is the speed of light (3 x 108 m/s). λ (nm) = 1241/ E (eV), where 1 eV equals to 1.062x10-19 J. Plants utilize the solar energy to fix atmospheric carbon dioxide and produce carbohydrates and oxygen by photosynthesis. The utilization of solar energy for wastewater treatment is an upcoming research field and needs special attention.

Mechanism of Photocatalysis

The solar energy can be harvested using different semiconductors (photocatalysts) for various applications such as solar panels, water splitting, and decontamination of pollutants from water [2]. A catalyst consists of an electron-filled valence band (Ev) and an empty conduction band, and the gap between these two is called band gap energy (Eg). The Fermi energy level (EF) of a semiconductor is referred to as the energy level at which the probability of occupation by an electron is one half. The band gap is larger in the insulator (> 4 eV), lesser in the semiconductor (1 < Eg < 4) and the two bands overlap in a metal. When a photon with an energy of hν matches or exceeds the Eg, an electron in the valence band is promoted to the conduction band, leaving a positive hole in VB. The reactive species, h+ and e− are powerful oxidizing and reducing

*Correspond author E-mail address: *priyankasave1984@gmail.com*

Harijan et al., (2025) Advances in Photocatalysis: Principles, Materials and Applications, https://doi.org/10.5281/zenodo.17214178

agents, respectively. Most of the photocatalysts work well absorbing wavelengths in the near-UV region (i.e. 390 nm), which is about 5% of the solar spectrum. Current efforts in the field are being devoted to optimizing the efficiency of these processes in the visible region (400 nm < λ > 750 nm) in many ways, such as doping with transition metal cations and nonmetal anions to produce intermediate states in the band gap [3], spectral sensitization using dye or polymer [4] and attaching photosensitizers such as another small band gap semiconductor or organic compounds that absorb visible light [5]. The photocatalytic activity of semiconductor photocatalysts is limited by the aggregation of nanoparticles and increases on the formation of mesoporous particles [6]. The charge recombination and separation/migration are two important competitive processes inside the semiconductor photocatalyst that largely affect the efficiency of the photocatalytic reaction [7].

Different types photocatalyst materials

The degradation process under solar irradiation: the conduction band edge of a semiconductor should be located above the reduction potential of water and the valence band below the oxidation potential. These are favorable for electron and hole transfer to oxidize water to oxygen.

Hematite (α-Fe2O3)

It is one of the important minerals of iron oxides and crystallizes in a rhombohedral lattice system. Hematite (α-Fe2O3) is a thermodynamically stable crystallographic phase of iron (III) oxide. It is abundant in earth's crust, low cost, and non-toxic. It has industrial applications as a red pigment [8], an anti-corrosion agent, and in electrochromic devices [9]. It is a semiconducting material with the negative temperature coefficient of resistance and the band gap of about 2 eV [10]. Hematite nanoparticles showed weak photocatalytic activity in solar light due to the high electron-hole combinations [11].

Zinc oxide, ZnO,

It is an n-type semiconductor due to oxygen vacancies or zinc interstitials. It crystallizes in the rocksalt or Rochelle salt, hexagonal wurtzite, and cubic zinc blende. The wurtzite structure is the thermodynamically most stable phase at ambient conditions. The zinc blende structure can be stabilized only by hetero-epitaxial growth substrates with cubic lattice structure. The rocksalt or Rochelle salt (NaCl) structure can be synthesized at high pressures (~10GPa). The wurtzite structure has a hexagonal unit cell with two lattice parameters, a and c, in the ratio of c/a = 1.6 (the ideal value for a hexagonal cell c/a = 1.633). Zinc oxide is a non-toxic n-type semiconductor with a large bandgap, 3.2 eV, and works well in UV light. The electron mobility of ZnO is temperature dependent and has a maximum of ~2000 cm2/(V·s) at 80 K, and hole mobility is in the range of 5-30 cm2/(V·s). The n-type doping is easily achieved, but p-type doping remains difficult due to the low solubility of dopants. It can be produced on a large scale at low cost [12].

The following is how the photocatalyst can be used; that is,

Degradation of methylene blue dye by photocatalytic activity of zinc oxide

Introduction

Many textile industries consumed different types of dyes in the coloring of yarns, fibers, and fabrics [1]. Thereby, the waste generated from the textile industry is discharged into the land and water without proper treatment. This is polluting the local environment and transmitting many diseases like allergic dermatitis, increased heart rate, vomiting, cyanosis, tissue necrosis, tumors, and enzyme disorders [2]. Various methods have been reported for effective removal of dyes from contaminated water [3]. Among them, adsorption and photocatalysis played a very important role in the water treatment. The regeneration of the adsorbents and storage of toxic sludge are the two major challenges in the adsorption process. Water purification via semiconductor photocatalysis is an environmentally friendly and inexhaustible process that converts dyes into gaseous products and does not pile up toxic sludge [4]. A photocatalyst absorbs photons with energy higher than its bandgap, causing electrons to jump into the conduction band and leaving holes in the valence band. These holes and electrons are powerful oxidants and reductants and decontaminate organic (or biological) and inorganic pollutants present in the water, respectively [5]. Solar energy is an unlimited source of renewable energy composed of 93% visible energy (> 380 nm) and 5%

ultraviolet energy (< 380 nm). The high band gap, rapid electron-hole recombination, and weak semiconductor-pollutant interaction are the key challenges that need to be overcome for the effective harvesting of solar energy for different applications [6-10]. Zinc oxide (ZnO) is an n-type semiconductor with a band gap of 3.2 eV, environmentally friendly, can be produced on a large scale, and has high carrier mobility [11-15]. Here we synthesized ZnO-based material via a chemical route and used it for the degradation of methylene blue (MB) dyes present in the water using solar energy.

Materials and Chemicals

All chemical reagents were purchased of analytical grade and used as such without any further purification. Zinc chloride (Sigma Aldrich, Bangalore, India), oxalic acid (Fisher Scientific, Mumbai, India), and sodium hydroxide (Fisher Scientific, Mumbai, India), methylene blue (Sigma Aldrich, St Louis, MO, USA), and ethanol (Merck, Mumbai, India) were used in the different experiments. The distilled water was used as a solvent for performing experiments and washing the products.

Synthesis of Zinc Oxide

Synthesis of ZnO was carried out by a chemical co-precipitation process. 3.0 g zinc (II) nitrate was dissolved in 100 ml water, and 4.0 g sodium hydroxide was dissolved in 100 ml water separately. The solutions were mixed in the 500 ml beaker, and after 1 hour of stirring at room temperature, a white-colored zinc oxide complex precipitated. The precipitate was washed with water and ethanol and dried at 100°C in an oven for 24 hours. The dried zinc hydroxide was calcined at 550°C for 3 hours.

Photocatalysis Experiments of Methylene blue

30 ppm stock solution was prepared by dissolving 7.5 mg methylene blue (MB, $C_{16}H_{24}C_lN_3O_3S$, molecular weight = 373.896 g/mol) in 250 ml distilled water and diluted further when needed. All batch experiments were carried out by mixing 10 mg of photocatalyst in 10 ml of MB dye solution. The adsorption was carried out in the dark for 2 hours to attain equilibrium between the photocatalyst and dye. The degradation of methylene blue was investigated in the solar light, and all the experiments were performed on the same day and time. The supernatant of the suspension was collected by centrifuging for 5 minutes. The concentration of methylene blue was analyzed using a UV-Vis spectrophotometer at the absorption band of 620 nm. Amount of methylene blue degraded at time 't' was calculated using the following equation: $(C_0\text{-}C_t)/C_0$, where C_o initial concentration and C_t represents the concentration at any time.

Analysis Instruments

The powder X-ray diffraction patterns (XRD) were recorded on a Bruker with Cu-Kα irradiation (λ = 1.5406 A˚) [16]. UV-visible spectra of the samples were obtained using a spectrometer in the wavelength region between 200 and 800 nm.

Result and Discussion

The powder X-ray diffraction patterns of ZnO are shown in the Figure 1. The powder XRD spectra of ZnO materials show peaks at 2θ, 31.76 (100), 34.40 (002), 36.25 (101), 47.57 (102), 56.77 (110), 62.89 (103), 66.41(200), 67.92 (112) and 69.02 (201), indicating the formation of crystalline zinc oxide with a hexagonal wurtzite structure (JCPDS 5-0664).

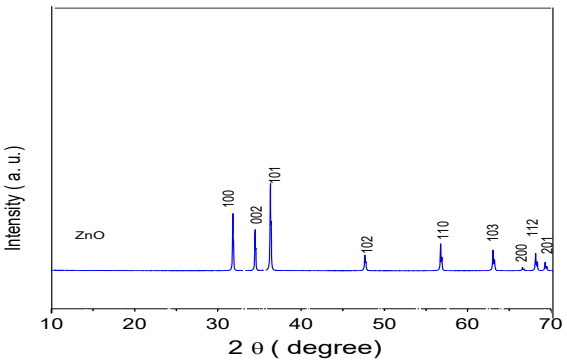

Fig 1: XRD image of ZnO

Degradation of methylene blue

In the typical experiment, 4 mg photocatalyst was dispersed in 10 ml of methylene blue solution (30 ppm), and adsorption capacity was tested in the dark for 2 hours to achieve equilibrium between dye and photocatalyst. Further photocatalytic activity was carried out under solar light for 2 hours. The decolorization process was monitored and quantified

by measuring the decrease in the intensity of absorption peaks of the dye solution and is shown in Figure 2.b for degradation in the solar light. The intensity of the dye absorption peak diminishes continuously with time without any shift in the band position (λmax). It indicates direct breakage of the dye molecule to the gaseous (CO2) product without the formation of other derivatives. This decrease in the adsorption capacity can be explained in terms of electrostatic and weak van der Waals interactions between the surface of the photocatalyst and the methylene blue dye molecule. Zinc oxide is a weak base, insoluble in water, and mainly exists as Zn(OH)+ at pH< 7[17]. In aqueous solution, the sulfonic group of methylene blue dissociates and forms anionic species MB (–SO3-). The adsorption capacity of MB in the highly loaded zinc oxide samples is higher because of the high electrostatic attraction between the negatively charged functional groups of MB (–SO3-) and positively charged Zn(OH)+. The degradation of dye was carried out in the sunlight at pH 7. When solar light irradiation on the methylene blue dye (MB) solution containing photocatalyst results in the excitation of dye molecule (MB)*. The excited dye injected the electrons into the conduction band (CB) of the photocatalyst, and the dye converted to a cationic free radical. Now injected electrons from MB* to ZnO and makes large charge separation. The dissolved oxygen in water captured electrons and produced highly reactive oxygen radicals (·-O2) and finally formed hydroxyl radicals (·OH). These oxygen (·-O2) and hydroxyl (·OH) radicals carried out degradation of methylene blue dye to CO2 and salt. Such type of mechanism has been discussed in the case of solar degradation of methylene blue using SnO2/graphene composite [18].

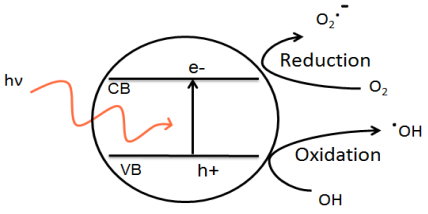

Fig 2 : (a) Photocatalytic activity

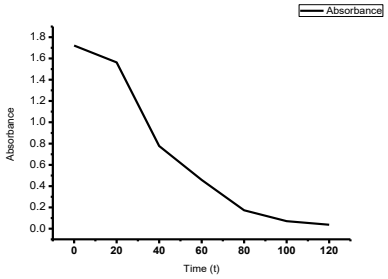

(b) Time-dependent adsorption of methylene blue dye on to ZnO

Effect of Adsorption Time

The time-dependent adsorption of methylene blue dye onto ZnO was studied for 30 ppm dye solution at pH 7.0 and 308 K and adsorbent dose 1.0 mg/mL. The time-dependent results showed that adsorption capacity increases with an increase in contact time and attains equilibrium after 120 min [Figure 2.b]. The adsorption capacity of ZnO was found to be 2.783 mg/g of 30 ppm methylene blue dye in 120 minutes.

Conclusion

Zinc oxide materials were synthesized successfully via precipitation of Zn^{2+} ions in a basic medium. The powder X-ray diffraction pattern images confirm the formation of the photocatalyst. The photocatalytic efficiency was evaluated towards degradation of methylene blue and found to be 2.783 mg/g of 30 ppm methylene blue dye in 120 minutes. This ZnO photocatalyst is expected to provide new pathways for the large-area fabrication of thin-film panels for the treatment of textile effluents using natural sunlight.

Acknowledgments

Thanks to Abhinav College of Arts, Commerce and Science, Bhayandar, Thane and the Sophisticated Instruments Center (SIC); and the Department of Chemistry at Dr. Harisingh Gour University for different characterizations/measurements of the samples.

References

1. J. Weber, V. C. Stickney. Wat.Res. 1993, 27, 63-67 (b) C. Ràfols, D. Barceló. J. Chromatogr. A 1997, 777, 177-192 (c) A. Houas, H. Lachheb, M. Ksibi, E. Elaloui, C. Guillard, J. M. Hermann. Appl. Catal. B: Environ. 2001, 31, 145-157.
2. U. Pagga, D. Bruan. Chemosphere 1986, 15, 479-491 (b) A. BiancoPrevot, C. Baiocchi, M. C. Brussino, E. Pramauro, P. Savarino, V. Augugliaro, G. Marci, L. Palmisano. Environ. Sci. Technol. 2001, 35, 971-976
3. T. Robinson, G. McMullan, R. Marchant, P. Nigam.Bioresource Technol. 2001, 77, 247-255.
4. Y. Qu, X. Duan.Chem. Soc. Rev. 2013, 42, 2568-2580.
5. M. R. Hoffmann, S. T. Martin, W. Choi, D. W. Bahnemann. Chem. Rev. 1995, 95, 69-96.
6. A. Fujishima, K. Honda. Nature 1972, 238, 37-38; M. A. Fox, M. T. Dulay.Chem. Rev. 1993, 93, 341-357 (b) Y. H. Zheng, C. Q. Chen, Y. Y. Zhan, X. Y. Lin, Q. Zheng, K. M. Wei, J. F. Zhu. J. Phys. Chem. C 2008, 112, 10773-10777 (c) R. Marschall. Adv. Funct. Mater. 2014, 24, 2421-2440.
7. R. M. Cornell, U. Schwertmann. 1st ed.; VCH Verlagsgesellschaft: Weinheim, Germany, 1996 (b) J. B. Fei, Y. Cui, J. Zhao, L. Gao, Y. Yang, J. B. Li. J. Mater. Chem. 2011, 21, 11742-11746.
8. G. Liu, Q. Deng, H. Wang, D. H. Ng, M. Kong, W. Cai, G. Wang. J. Mater. Chem. 2012, 22, 9704-9713.
9. A. M. Mansour. RSC Adv. 2015, 5, 62052-62061.
10. W. F. Tan, Y. T. Yu, M. X. Wang, F. Liu, L. K. Koopal. Cryst.Growth Des. 2014, 14, 157-164.
11. Z. Zhang, M. F. Hossain, T. Takahashi. Appl. Catal. B 2010, 95, 423-429.
12. P. Basnet, G. K. Larsen, R. P. Jadeja, Y. C. Hung, Y. Zhao. ACS Appl. Mater. Interfaces 2013, 5, 2085-2095.
13. S. D. Tilley, M. Cornuz, K. Sivula, M. Grätzel. Angew. Chem. Int. Ed. 2010, 49, 6405-6408.
14. M. A. Ahmeda, E. E. El-Katori, Z. H. Gharni. J. Alloy Compd. 2013, 553,19-29.
15. R. Kumar, S. Anandan, K. Hembram, T. N. Rao. ACS Appl. Mater. Interfaces 2014, 6, 13138-13148.
16. R. Wahab, S. G. Ansari, Y. S. Kim, H. K. Seo, G. S. Kim, G. Khang, H. S. Shin. Mater. Res. Bull. 2007, 42, 1640- 1648
17. S. W. Bian, I. A. Mudunkotuwa, T. Rupasinghe, V. H. Grassian.Langmuir 2011, 27, 60596068 (b) A. C. Lucilha, C. E. Bonanceˆa, W. J. Barreto, K. Takashima.Spectrochim.Acta. Part A Mol. Biomol. Spectrosc. 2010, 75, 389-393.
18. H. Seema, K. C. Kemp, V. Chandra, K. S. Kim. Nanotechnology 2012, 23, 355705-355711.